[10]D. Liberman, J. T. Waber, and D. F. Cromer (a personal communication referenced in Seaborg's paper).

[11]R. D. Cowan, Phys. Rev. 163, 54 (1967).

[12]J. C. Slater, Intern. J. Quantum Chem. 1s, 783 (1967).

[13]T. Koopmans, Physica 1, 104 (1934).

[14]The self-consistency criteria finally used are as follows: For $Z < 50$ the solution was considered self-consistent when the change in $r_i V_i(r)$ was less than five parts in 10^7 from one primary iteration cycle to the next, and the secondary iteration on the eigenvalues (during each primary cycle) was discontinued when $\Delta\epsilon_i/\epsilon_i$ was less than five parts in 10^{10}. For $Z \geq 50$ the change in $r_i V_i(r)$ was made less than one part in 10^8 and the eigenvalue change was required to be less than one part in 10^{11}.

[15]Perturbations of $sd\,{}^1D$ by $p^2\,{}^1D$ in Be, Mg, Ca, Sr, and Ba, and of s^2d by $sp^2\,{}^2D$ in B, are well known, and in most cases are of the proper sign and magnitude to account for much of the apparent error.

[16]These two possible alternatives are the source of considerable convergence difficulties in SCF iterations for certain configurations.

[17]An example can be seen by comparing the potential (Fig. 4) for La I $6s5d5f$ (the f electron *outside* the $6s$ and $5d$ electrons) with that (Fig. 3) for La I $4f6s5d$ (the f electron *inside* the $6s$ and $5d$). Clearly the difference between the $4f$ potentials for Ba and La in Fig. 3 is due primarily to this relaxation effect.

[18]The existence of abrupt changes in n^* for d electrons has of course long been known experimentally.

[19]A. R. P. Rau and U. Fano, Phys. Rev. 167, 7 (1968).

[20]The HX potentials show double-well structures as early as Al I $3s^23d$ ($\langle r\rangle_{3s} = 2.44$); the inner well becomes successively deeper and the potential barrier successively higher as the $3s^23p^m$ core contracts with increasing Z (and m), until this core is completed at K I $3p^63d$ ($\langle r\rangle_{3p} = 1.43$). The most pronounced barrier (extending to positive energies) appears in the configuration Cu I $3d^{10}4d$ ($\langle r\rangle_{3d} = 0.98$).

[21]See, for example, B. Edlén, Handbuch der Physik, edited by S. Flügge (Springer-Verlag, Berlin, 1964), Vol. XXVII, pp. 91f; or B. G. Wybourne, Spectroscopic Properties of the Rare Earths (Interscience Publ., New York, 1965), pp. 1–4.

[22]The experimental shape of the quantum-defect curve of Ba II, completely different from the flat ($n - n^*$ = integer) curves for nf series in neutral atoms, is thus easily understandable, and is *not* due to perturbations such as those suggested by E. Rasmussen, Z. Physik 83, 404 (1933). [See also V. Kaufman and J. Sugar, J. Res. Natl. Bur. Stand. 71A, 583 (1967).].

[23]R. D. Cowan, J. Opt. Soc. Am. 58, 924 (1968).

[24]Computed values of F^2 for the super-actinides are approximately 0.3, 0.6, and 1.3 Ry for $7d$, $6f$, and $5g$ electrons, respectively.

[25]R. D. Cowan, J. Opt. Soc. Am. 58, 808 (1968).

[26]A. Giacchetti, J. Opt. Soc. Am. 56, 653 (1966); B. Osman and J. Blaise, unpublished.

PHYSICAL REVIEW VOLUME 177, NUMBER 1 5 JANUARY 1969

Measurement of the Total Cross Section for Symmetric Charge Exchange in Helium from 400 - 2000 eV*

Stephen W. Nagy, William J. Savola, Jr., and Edward Pollack
Physics Department, University of Connecticut, Storrs, Connecticut
(Received 19 June 1968)

The energy dependence of the total cross section for symmetric charge exchange in helium is measured in the range from 400–2000 eV. Beam-attenuation techniques are used, and all measurements are made on the forward-scattered ions and the high-energy neutrals resulting from the charge exchange. Cross-section values are given at 100–eV intervals, and the results show a cross section decreasing as the energy increases, with a value at 1000 eV of 1.04×10^{-15} cm^2. The absolute cross sections are accurate to ± 12%. Relative cross-section values accurate to ± 6% are reported.

INTRODUCTION

The $He^+ + He$ collision has been studied in great detail both experimentally and theoretically in recent years. These studies have led to a better understanding of the collision process and of the molecular states involved. In the energy region from several hundred to several thousand electron volts, the most significant contribution to the total cross section in $He^+ + He$ collisions comes from resonant charge exchange. Although there have been many studies of the total cross section for symmetric charge exchange in helium there is still a substantial lack of agreement among the published results.

The typical collision in the $He^+ + He \rightarrow He + He^+$ process involves very little kinetic-energy transfer between the partners. It is generally a glancing collision resulting in a high-energy neutral atom scattered in the forward direction and a low-energy ion recoiling in a perpendicular direction. The forward-scattered neutral atoms have nearly the same kinetic energy as the incident ions. The general feature of the resonant charge-exchange cross section is that it decreases with increasing energy, while nonresonant charge-exchange cross sections at first increase to a broad maximum and then decrease with increasing energy.[1]

There are basically two experimental methods available for charge-exchange measurements.[2] The first of these involves measurements on the low-energy recoil ions generated in a well-defined region of the scattering chamber. This is the most popular method used in the energy region studied by the present experiment. The second method involves direct measurements on the high-energy forward beam. The present experiment uses a modification of the second method suitable for resonant charge-exchange measurements in an energy region where the elastic and the noncharge-exchange inelastic scattering contributions to the total cross section are small.

The theoretical calculations of symmetric resonant charge-exchange cross sections are generally carried out by studying the process in three velocity ranges. The present results lie in the "intermediate" velocity range corresponding to velocities larger than 10^5 cm/sec and less than 10^8 cm/sec. In this energy range the theory reduces to one involving semiclassical impact-parameter techniques. For an ion of velocity v, and an impact parameter b, the probability of symmetric resonant charge exchange $P(b, v)$ is given by[3]

$$P(b, v) = \sin^2 \left(\int_{-\infty}^{+\infty} \frac{(E_g - E_u)}{2\hbar v} \, ds \right) . \qquad (1)$$

E_g and E_u are the gerade and ungerade electronic energies of the He_2^+ system and are functions of s, the internuclear separation along the collision orbit. The total cross section, $\sigma(v)$, is then obtained from

$$\sigma(v) = 2\pi \int_0^{\infty} P(b, v) b \, db \ . \qquad (2)$$

A comparison of the experimental results with theory serves the multiple purpose of checking the validity of the impact-parameter method as applied to the problem, as well as the appropriateness of the potentials selected.

THE EXPERIMENTAL METHOD

The energy dependence of the total cross section for the scattering of He^+ ions by He atoms is measured in an energy range from 400 – 2000 eV. Attenuation techniques are used and the cross section is obtained from the equation

$$I = I_0 e^{-n\sigma_t l} , \qquad (3)$$

where I is the attenuated He^+ current reaching the detector, I_0 the He^+ current reaching the detector with no scattering gas, n the target gas density, l the scattering path length, and σ_t the total cross section. The measured cross sections include contributions from charge-exchange collisions as well as from those elastic and inelastic scattering events resulting in ions scattered beyond the detector. Although there are presently no values available of the total cross section for such elastic scattering in this energy range, it is reasonable to expect that these cross sections will be small compared with that for charge-exchange scattering in the forward direction. The important inelastic channels have total cross-section values down by several orders of magnitude[4] from those obtained in the present experiment. The attenuation technique is therefore suitable for the measurement of the charge-exchange cross section, which to a good approximation is the measured cross section.

Figure 1 shows the experimental method used for the measurement. Helium gas at a pressure of about 10^{-2} Torr is admitted to an electron-impact ion source floated at the required voltage. The ions formed are extracted from the source and pass through an ion-optics and mass-spectrometer system. After suitable collimation the ion beam enters the scattering chamber and is partially neutralized. The resulting beam consisting of ions and neutrals is again collimated and detected. The experiment is performed by measuring the unattenuated He^+ current I_0, a current I_A arising from the attenuated He^+ beam and high-energy He, and I_N the current resulting from secondary electron emission from the detector due to high-energy He only. The attenuated ion

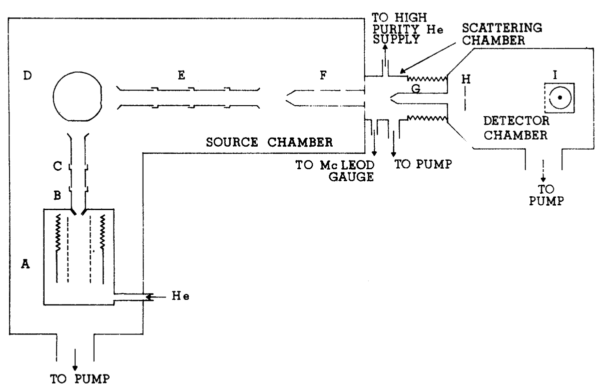

FIG. 1. A schematic diagram showing some of the important experimental details. Helium is fed by a gas handling system to the ion source (A) where it is partially ionized by collisions with electrons. The ions are extracted from the source by an extractor (B) and are focused at a suitable point in front of the mass-spectrometer magnet (D) by the ion optics (C). The mass analyzed beam is then collimated by additional ion optics (E) and goes through a hole centered on a button inserted on the left side of the button holding cylinder (F). After passing through a second hole on the right side of the cylinder the collimated beam enters the scattering chamber containing helium at low pressure. As a result of charge-exchange collisions the beam is partially neutralized. The scattering region is terminated by a snout (G) containing a collimating hole. The beam passes through another hole (H) and a grid to the detector (I). The experiment is performed by measuring the beam current with and without scattering gas. The cross sections are obtained from a knowledge of the apparatus geometry and the scattering gas pressure.

current I in Eq. (3) is equal to $I_A - I_N$. The neutral component is selected by the use of a bias voltage on a grid placed in front of the detector. Cross sections are obtained from Eq. (3) which can be rewritten at room temperature as

$$\sigma(v) = \frac{3.10\times 10^{-17}}{lp} \ln\left(\frac{I_0}{I_A - I_N}\right) \mathrm{cm}^2 , \qquad (4)$$

where p is the scattering gas pressure in Torr. Relative cross sections are found by comparing the $\ln[I_0/(I_A - I_N)]$ at the various energies to the value of this expression obtained at 1000 eV. The cross section at 1000 eV is determined after an absolute pressure measurement is made with the aid of a McLeod gauge.

The experimental method used offers the distinct advantage of making all the required measurements on the forward-scattered beam, thus allowing a direct study of the high-energy neutrals. Since the detector is in the forward direction, beam profiles are easily obtainable, and the symmetry and location of the ion and neutral beams can be checked. This makes it possible to determine whether stray charges (which are always present in experiments involving ion beams) are influencing the measurement since their presence in critical areas would result in beam asymmetries or a relative displacement of the neutral and ion beams.

THE APPARATUS

The vacuum system is constructed from stainless steel and consists of source, scattering, and detector chambers. The scattering chamber is connected to the detector chamber by a bellows enabling the detector to rotate about a fixed point in the scattering chamber. This motion enables beam profiles to be taken and makes possible a precise alignment of the detector and beam during the experiment.

The He^+ beam is obtained from an electron-impact ion source. The source consists of a stainless-steel water-cooled jacket and a removable flange on which there are mounted a cylindrical grid structure and an assembly holding two tungsten filaments (one serving as a spare) just outside the grid. It is well known that experimental cross-section values may be influenced by the ion source used since excited ions may be produced in the source. To check the present ion source for possible effects on the measurements, attenuation measurements are made using He^+ ions formed by ionizing collisions with electrons of different energy. The results are independent of electron energy to well within the accuracy of the experiment. As an example, at 1000-eV He^+ energy a ratio of $I_0/I = 1.173$ is obtained when 50-V electrons are used for ionization. The value of this ratio obtained with 150-V electrons agrees with this number to within 0.1%. Although only 65-V electrons are required to excite the metastable ion state, it may be concluded that this state does not influence the determination of the cross section when 150-V electrons are used. The data are taken using 150-V electrons which results in a higher beam intensity at a slight cost in the beam-energy spread. With 150-V electrons the energy spread in the ion beam is measured to be ±5 eV. This value is obtained by the use of a retarding potential on a grid in front of the detector.

As shown in Fig. 1 the He^+ ions are extracted from the source and pass through an ion-optics and mass-spectrometer system. The ion-optics system consists of a set of cylindrical aluminum lenses designed to shield the beam from the rest of the apparatus whenever possible. Since the scattering chamber is grounded it is necessary to float the ion source at the required voltage and, in addition, to maintain the correct relative voltages between the various components. This is accomplished by using a well-regulated power supply to float the ion source, and by using an identical unit to supply a voltage divider network which is connected to the various lenses and to the mass analyzing magnet. After leaving the ion-optics system the beam is collimated by a 0.157-cm-diameter hole, centered in a button which is inserted in cylinder F (Fig. 1) and by a 0.089-cm-diameter hole in a second button similarly mounted at the opposite end of the 8-cm-long cylinder. The beam then enters the scattering chamber which is supplied with ultrapure ionization grade helium. The pressure in the scattering region can be monitored continuously by a nude ionization gauge as well as by a conventional Bayard-Alpert type in a glass bulb. In addition an absolute pressure measurement can be made with a McLeod gauge which is connected to the scattering chamber through a liquid nitrogen trap. The scattering region is terminated by a snout (G in Fig. 1) which is fitted with a button containing a 0.046-cm-diameter hole at its center. Collimation of the scattered beam is achieved by using this hole in conjunction with a second hole 8 cm away, of diameter 0.089 cm (H in Fig. 1) resulting in an acceptance angle of ±0.5°.

Although determinations of the relative cross sections are independent of the length of the scattering path and scattering pressure in the present experiment, an absolute determination of the cross section requires a knowlege of these. Since the scattering gas is not confined to a path length l in the scattering chamber, a correction to Eq. (4) is required. This additional scattering may be accounted for by replacing l by $(l + \Delta l)$ in the equation. For the particular geometry used, a good approximation to Δl may be obtained from a comparison of the pressures in cylinder F and snout G to the pressure in the scattering chamber. For a gas of density n molecules/cm³ having a mean molecular velocity $\langle v\rangle$, the kinetic theory of gases shows that $\frac{1}{4}n\langle v\rangle A$ molecules per second effuse through a thin-walled aperture of area A. In the steady state the number of helium atoms per second entering cylinder F from the scattering chamber must be equal to the number pumped out into the general vacuum system through a set of pumping holes provided on the cylinder. Assuming equal temperatures in the scattering chamber and cylinder, the density of helium in the region of the cylinder, n_C, is given by $n_C = nA/A_C$ where A_C is the total pumping area on the cylinder and A the area of the appropriate collimating hole. The attenuation of the ion signal in the cylinder then depends on the product $n_C l_C = n\Delta l_C$ where l_C is the length of the cylindrical region and Δl_C is the equivalent length at scattering-chamber pressure. A similar calculation is made for the snout region and both terms are added to yield $\Delta l = 0.058l$. The effective length of the scattering chamber $l + \Delta l$ for the present apparatus is 1.868 cm.

The detector consists of a section of tantalum wire surrounded by a conducting chamber containing a small slit to admit the beam. The wire is connected to an electrometer which measures the resulting currents. These currents are generated by the incident ions as well as by the secondary electrons resulting from the impact of the ions and neutrals on the tantalum surface. As Fig. 2 shows, a grid placed directly in front of the detector can be biased to pass a beam consisting of ions and neutrals or neutrals alone. The curve labeled A shows an X-Y recorder plot of the detected current versus scattering gas pressure at a beam energy of 850 eV with a grid bias of 840 V. The detected current decreases with increasing pressure indicating the attenuation of an ion signal. The high-energy neutral component formed from charge-exchange collisions is of course present but its effect on the current is masked by the large ion signal. The curve labeled B is taken at the same beam energy but with a grid bias of 860 V. The detected current increases with increasing pressure and shows that the high-energy neutrals are detected. The scale for curve B is multiplied by a factor of 10 relative to that for curve A. Although the electric fields of the grid may affect the collection efficiency of the detector, the cross sections are independent of such effects since only ratios of currents are required for cross-section determinations. High angular resolution is not desirable in total charge-exchange cross-section experiments of this type, since ions which are elastically scattered beyond the detector would contribute to the cross section. Beam-profile studies, however, require high angular resolution, and since these profiles serve as an important check on the data obtained it was considered essential to use a detection system which could satisfy both of the angular-resolution requirements. An angular resolution of $\pm 0.5°$ was selected for the cross-section determination. This was sufficiently low so that the effects of elastic scattering are small and yet suitable to provide some beam-profile information. The acceptance angle of the detector is determined by holes G and H (Fig. 1). The tantalum wire, which serves as the beam collector, has a diameter of 0.038 cm which together with hole G increases the angular resolution to $\pm 0.2°$. All the ions going through holes G and H are, however, collected by this wire since it is at the lowest potential in the detector circuit and the ions essentially move along field lines terminating on the wire. During the runs the conducting chamber surrounding the wire is electrically connected to the grid. As a check on the collection efficiency of the wire the chamber is at times disconnected from the grid and connected to the wire to provide a large collecting surface. The currents due to the wire alone and the wire and chamber together are compared and are found to be essentially the same. This indicates that the wire does not change the $\pm 0.5°$ angular resolution for the ion beam. For the neutrals, however, the angular resolution is increased to $\pm 0.2°$ since the neutrals are not affected by the electric fields. This feature provides more accurate profiles of the neutral beam and is worthwhile since such information is useful in the planning of high-energy neutral-beam-scattering experiments.

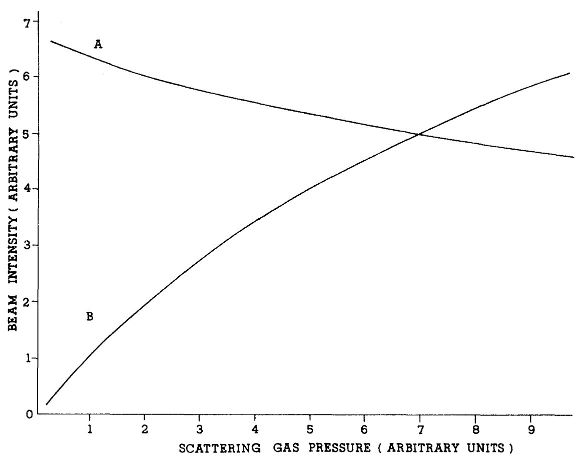

FIG. 2. The effect of grid bias voltage on the type of signal reaching the detector. The curve labeled A shows an X-Y recorder plot of the detected current versus scattering gas pressure at a beam energy of 850 eV with a grid bias of 840 V. The detected current decreases with increasing pressure indicating the attenuation of an ion signal. The high-energy neutral component formed from charge-exchange collisions is of course present but its effect on the current is masked by the large ion signal. The curve labeled B is taken at the same beam energy but with a grid bias of 860 V. The detected current increases with increasing pressure and shows that the high-energy neutrals are detected. The scale for curve B is multiplied by a factor of 10 relative to that for curve A. The attenuated ion signal may be obtained by subtracting curve B from curve A after a suitable correction is made for the differences in scale.

THE RESULTS

Table I shows the relative charge-exchange cross sections normalized to the value of the cross section at 1000 eV. The table represents data taken over a period of three months and the relative results are reproducible to $\pm 6\%$. The determination of the relative cross sections requires alternate measurements of the beam at zero scattering pressure (for I_0) and at an arbitrarily fixed scattering pressure p (for I). All runs are made at different arbitrarily selected pressures in the single collision region (as determined from beam intensity versus scattering-pressure curves). Assuming constant scattering pressure during a run, the relative cross section at a given energy is obtained by dividing $\ln(I_0/I)$ at the required energy by its value at 1000 eV. The pressure is reset to within

TABLE I. Relative charge-exchange cross sections normalized to the cross section at 1000 eV. The relative results are accurate to ± 6%. The absolute cross sections may be found by multiplying the relative values by the cross section at 1000 eV which is determined to be 1.04×10^{-15} cm^2. The absolute results are accurate to ± 12%.

Energy (eV)	Relative cross section
400	1.37
500	1.25
600	1.13
700	1.09
800	1.04
900	1.01
1000	1.00
1100	0.994
1200	0.969
1300	0.963
1400	0.940
1500	0.931
1600	0.934
1700	0.874
1800	0.893
1900	0.865
2000	0.893

one part per hundred during each set of runs, and the average standard deviation in the ratio (I_0/I) at any energy is less than 1% of the ratio. In order to verify that stray charge buildup is not influencing the data, the zero position of the beam is checked frequently. Figure 3 shows typical profiles of the combined ion and neutral beam and of the neutral beam alone. These profiles are taken at a beam energy of 2000 eV, and the scale for the neutral beam intensity is multiplied by a factor of 20 relative to the units shown. Reproducible data are obtainable if the profiles are symmetric and there is no relative displacement between them (stray charge in critical regions would result in such displacements). All runs are made with a maximum energy spread of ± 5 eV.

The absolute cross sections may be found by multiplying the relative values in Table I by the absolute cross section at 1000 eV which is determined to be 1.04×10^{-15} cm^2. The values obtained are accurate to ± 12%. As in most scattering experiments the largest single source of error is due to uncertainties in the scattering gas pressure. Figure 4 shows the present results compared with those of some of the more recently published studies. Solid lines represent theoretical calculations and the points are experimentally determined values. The present results are represented by the circles, those of Hayden and Utterback[5] by squares, and the results of Hasted and Stedeford[6] by triangles. The presently obtained 1000-eV point is in exact agreement with that of Ref. 5. The present results are also in agreement with those of Moiseiwitsch (M).[7] Reference 7 gives results using three different approximations and the one reproduced in Fig. 4 represents a calculation using a two-parameter helium-atom wave function. The Rapp and Francis[3] prediction (RF) falls below the present results while those of Iovitsu and Pallas[8] (IP) as modified in Ref. 3 are still lower.

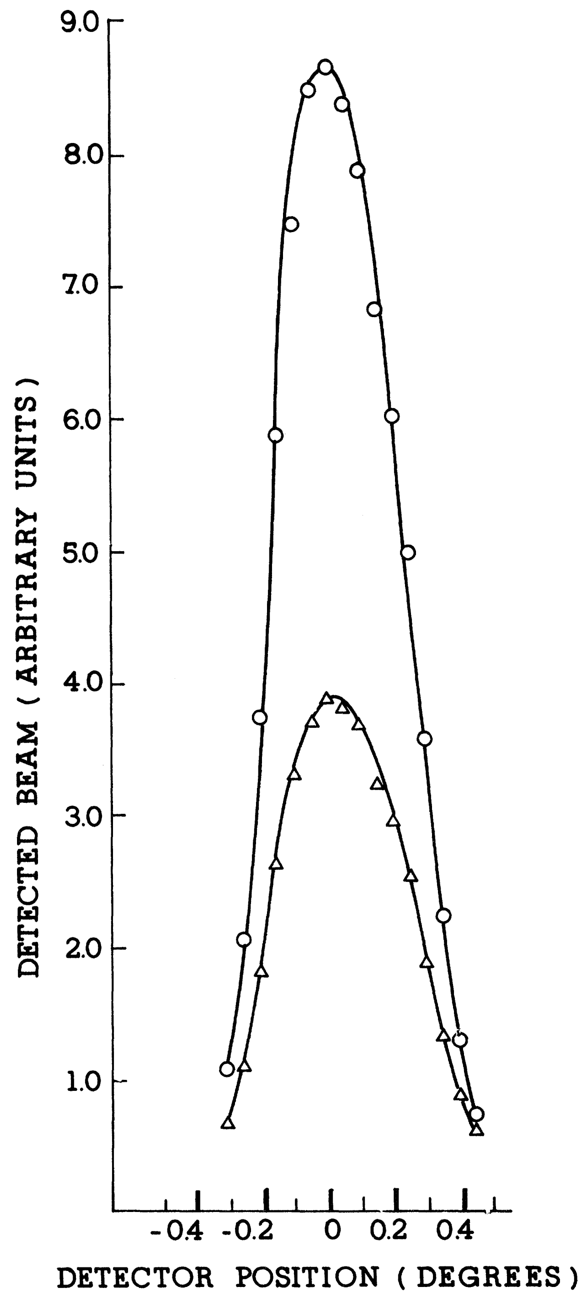

FIG. 3. Typical beam profiles. The plot shows a profile of the combined ion and neutral beams (upper curve) and the neutral beam alone at an energy of 2000 eV. The combined ion and neutral profile is obtained with a grid bias of 1990 V and the neutral profile with a grid bias of 2010 V. The neutral beam intensity is multiplied by a factor of 20 relative to the units shown. Reproducible data are obtained if the profiles are symmetric and there is no relative displacement between them.

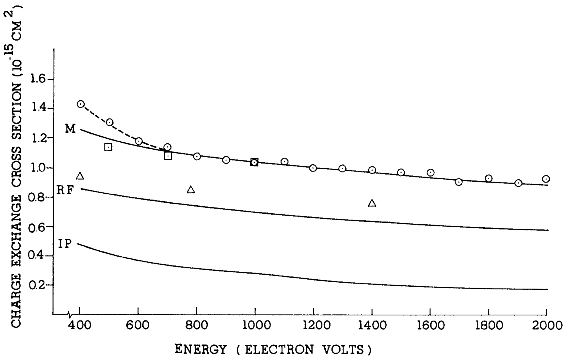

FIG. 4. The experimental results showing the total cross section for symmetric charge exchange in helium as compared with those of some of the more recently published studies. Solid lines represent theoretical calculations and the points represent experimental determinations. The results of the present experiment are represented by circles, those of Hayden and Utterback (Ref. 5) by squares, and those of Hasted and Stedeford (Ref. 6) by triangles. The solid curves represent the calculations of Moiseiwitsch (M) (Ref. 7), Rapp and Francis (RF) (Ref. 3), and of Iovitsu and Pallas (IP) (Ref. 8) as modified in Ref. 3.

The results obtained show that above 600 eV the assumption made about elastic scattering is reasonable. In addition the neutral beam profile in Fig. 3 shows that complex scattering experiments with high-energy neutrals are indeed possible. For such experiments the neutral beam intensity could be substantially increased by operating a charge-exchange region at higher pressures than used in the present experiment. The first dynode of a multiplier could also replace the tantalum wire as the neutral beam detector.

ACKNOWLEDGMENTS

The authors wish to thank Professor Edgar Everhart for the many discussions with him during the course of the experiment. They are grateful to Frederick J. Eriksen and Salvador M. Fernandez for their assistance at times.

---

*This work was supported by the U. S. Army Research Office, Durham, and the University of Connecticut Research Foundation.

[1]J. B. Hasted, Physics of Atomic Collisions (Butterworths Scientific Publications, Ltd., London, 1964), Chap. 12.

[2]R. F. Stebbings, in Molecular Beams, edited by J. Ross (Interscience Publishers, Inc., New York, 1966).

[3]D. Rapp and W. E. Francis, J. Chem. Phys. 37, 2631 (1962).

[4]D. P. Sural, S. C. Mukherjee, and N. C. Sil, Phys. Rev. 164, 156 (1967).

[5]H. C. Hayden and N. G. Utterback, Phys. Rev. 135, A1575 (1964).

[6]J. B. Hasted and J. B. H. Stedeford, Proc. Roy. Soc. (London) A227, 466 (1955).

[7]B. L. Moiseiwitsch, Proc. Phys. Soc. (London) A69, 653 (1956).

[8]I. Popescu Iovitsu and N. Ionescu-Pallas, Zh. Techn. Fiz. 29, 866 (1959) [English transl.: Soviet Phys. – Tech. Phys. 4, 781 (1960)].